

Supporting Information

Mechanically Strong Superabsorbent Terpolymer Hydrogels Based on AMPS via Hydrogen-Bonding Interactions

Busra SEKIZKARDES^{1†}, Esra SU^{2}, and Oguz OKAY^{1*}*

¹Istanbul Technical University, Department of Chemistry, 34469 Maslak, Istanbul, Turkey.

² Istanbul University, Faculty of Aquatic Sciences, 34134 Fatih, Istanbul, Turkey

[†] Present Address: Turkish-German University, Department of Material Science and Technology,

34820, Beykoz, Istanbul, Turkey

* To whom correspondence should be addressed:

Oguz Okay

Department of Chemistry, Istanbul Technical University, Maslak, 34469 Istanbul, Turkey.

Tel: +90 212 285 3156

E-mail: okayoo@itu.edu.tr ORCID Oguz Okay: 0000-0003-2717-4150

Esra Su

Faculty of Aquatic Sciences, Istanbul University, 34134 Fatih, Istanbul, Turkey.

Tel: +90 539 301 2726

E-mail: esra.su@istanbul.edu.tr ORCID Esra Su: 0000-0001-6643-6788

Table of Contents

Table S1. The swelling ratio and mechanical parameters of the hydrogels.	S3
Table S2. The mechanical parameters of the hydrogels formed at various w .	S3
Table S3. Elemental microanalysis results of sol and gel phases.	S3
Table S4. The composition of sol and gel phases of the hydrogels.	S4
Table S5. The amount of the monomers and water in the preparation of hydrogels at $w = 25$ wt % and at various x_{MAAc} .	S4
Table S6. The amount of the monomers and water in the preparation of hydrogels at $x_{\text{MAAc}} = 0.80$ and at various w .	S5
Figure S1. (a) The images of the phase-separated hydrogel. $w = 95$ wt %. (b) Amide I region of the FTIR spectra of solution and gel phases.	S5
Figure S2. FTIR spectra of PAMPS, PMAAc, and PDMAA physical hydrogels.	S6
Figure S3. Five successive compressive cycles.	S7
Figure S4. Eight successive tensile cycles for the hydrogels prepared at $w = 40$ wt %.	S7
Figure S5. Eight successive tensile cycles for the hydrogels prepared at various w .	S8

Table S1. The swelling ratio and mechanical parameters of the hydrogels formed at various x_{MAAc} . $w = 25$ wt %. Standard deviations are given in parenthesis.

x_{MAAc}	m_{rel}	E / MPa	σ_f / MPa	ϵ_f %	W / MJ.m ⁻³
1.0	1400 (303)	5.3 (0.6)	4.0 (0.2)	316 (25)	11.9 (1.7)
0.8	2035 (255)	26 (2)	10.4 (0.7)	325 (42)	31 (5)
0.7	2063 (154)	23.2 (3.4)	11 (1)	237 (52)	26.9 (1.4)
0.6	2913 (134)	11.2 (2.1)	7.4 (0.8)	416 (46)	24.0 (2.2)
0.5	2613 (193)	10.5 (1.3)	7.1 (0.4)	703 (55)	44.4 (4.8)
0.4	2200 (15)	2.17 (0.2)	2.5 (0.3)	633 (50)	13.5 (1.5)
0.2	1710 (76)	1.12 (0.1)	1.2 (0.1)	388 (23)	4.5 (0.3)
0.0	1071 (75)	0.40 (0.05)	0.58 (0.05)	329 (30)	2.0 (0.4)

Table S2. The mechanical parameters of the hydrogels formed at various w . $x_{\text{AMPS}} = 0.80$. Standard deviations are given in parenthesis.

w %	E / MPa	σ_f / MPa	ϵ_f %	W / MJ.m ⁻³
25	26 (2)	10.4 (0.7)	325 (42)	30.8 (2.9)
30	1.6 (0.1)	2.2 (0.2)	517 (44)	8.7 (0.9)
40	0.36 (0.03)	0.30 (0.02)	249 (13)	0.72 (0.14)
50	0.17 (0.01)	0.12 (0.01)	169 (12)	0.18 (0.02)
75	7×10^{-3} (1×10^{-3})	0.015 (0.001)	456 (39)	0.063 (0.005)

Table S3. Elemental microanalysis results of sol and gel phases of the hydrogels formed at $w = 93$ and 95 wt%.

Location	w wt%	C wt%	N wt%	S wt%
Sol	95	42	5.74	8.7
	93	42.4	5.87	9.21
Gel	95	48.9	2.98	3.77
	93	45.9	4.41	6.36
In the feed		47.3	5.3	9.1

Table S4. The composition of sol and gel phases of the hydrogels formed at $w = 95$ and 93 wt%.

Location	w wt%	AMPS	DMAA	MAAc	x_{MAAc}
		mol %	mol %	mol %	
Sol	95	35.8	18.2	46.0	0.72
	93	38.9	17.9	43.2	0.71
Gel	95	12.0	9.7	78.3	0.89
	93	22.9	13.5	63.6	0.83
In the feed		38	12.4	49.6	0.80

Table S5. The amount of the monomers and water in the preparation of hydrogels at $w = 25$ wt % and at various x_{MAAc} . Irgacure = 15 mg.

x_{MAAc}	AMPS / g	MAAc / g	DMAA / g	Water / g
1.0	2.5	1.7	0	1.4
0.8	2.5	1.4	0.4	1.4
0.7	2.5	1.2	0.6	1.4
0.6	2.5	1.0	0.8	1.4
0.5	2.5	0.9	1.0	1.4
0.4	2.5	0.7	1.2	1.5
0.2	2.5	0.3	1.4	1.5
0.0	2.5	0	2.0	1.5

Table S6. The amount of the monomers and water in the preparation of hydrogels at $x_{\text{MAAc}} = 0.80$ and at various w . Irgacure = 15 mg.

w	wt%	AMPS / g	MAAc / g	DMAA / g	Water / g
25		2.5	1.4	0.4	1.4
30		2.5	1.4	0.4	1.8
40		2.5	1.4	0.4	2.9
50		2.5	1.4	0.4	4.3
80		2.5	1.4	0.4	17.2
90		2.5	1.4	0.4	38.7
95		2.5	1.4	0.4	81.7
99		2.5	1.4	0.4	425.7

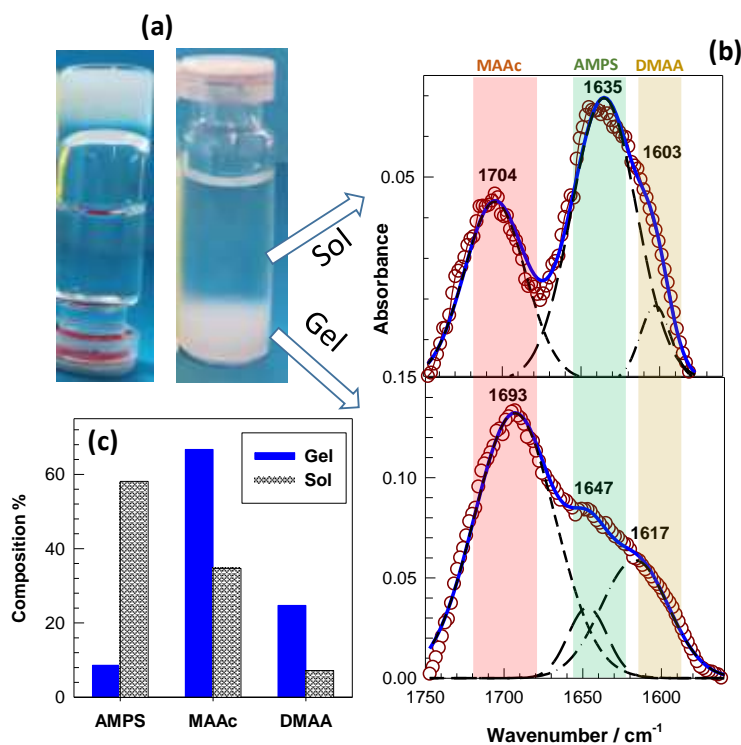


Figure S1. (a) The images of the phase-separated hydrogel. $w = 95$ wt %. (b) Amide I region of the FTIR spectra of solution (up) and gel phases (down) of the phase-separated hydrogel. The open symbols and blue solid curves present original and fitted spectra while black dashed lines are hidden peaks for MAAc (dashed), AMPS (long dash), and DMAA units (dash-dot). (c) The composition of the terpolymers in the sol and gel phases of the phase-separated hydrogel.

The C=O stretching vibrations of AMPS units in the sol and gel appear at 1635 and 1647 cm^{-1} , respectively, where the strong absorption peak for the sol reveals that it is rich in AMPS units. The C=O stretching of MAAC units appears at 1704 and 1693 cm^{-1} for sol and gel respectively. The absorption peak for the DMAA units cannot be detected in FTIR spectra although it appears in physical PDMAA hydrogels formed at $C_o = 50$ wt % and under identical conditions at 1603 cm^{-1} (Figure S2). To estimate the composition of the terpolymers in the gel and sol phases, their spectra were analyzed using PeakFit software. Linear baseline correction was applied to the amide I region (1560–1750 cm^{-1}) before the band was deconvoluted by Gauss Amplitude function. For the curve fitting procedure, the peak positions of MAAC and AMPS were fixed, allowing their widths and heights to vary. The peak position of the hidden peak of DMAA was varied to obtain a good fit to the spectra of the terpolymer with a r-squared value above 0.98. The open symbols and blue solid curves in Figure 6b present original and fitted spectra while black dashed lines are hidden peaks for MAAC (dashed), AMPS (long dash), and DMAA units (dash-dot). The composition of the terpolymers is estimated from the area of the peaks and presented in Figure 6c. It is seen that the terpolymer in the sol phase consists of 58 mol % AMPS compared to 9 mol % in the gel, which is responsible for its water solubility due to the osmotic pressure of AMPS counterions dominating the elastic response of physical cross-links. Moreover, in contrast, the polymer in the gel phase is rich in both MAAC and DMAA units. We should note that FTIR analysis can give only qualitative analysis of the polymers without standards which are hard to prepare for the present terpolymers. Therefore, elemental analysis for C, N, and S was performed as detailed in the texts.

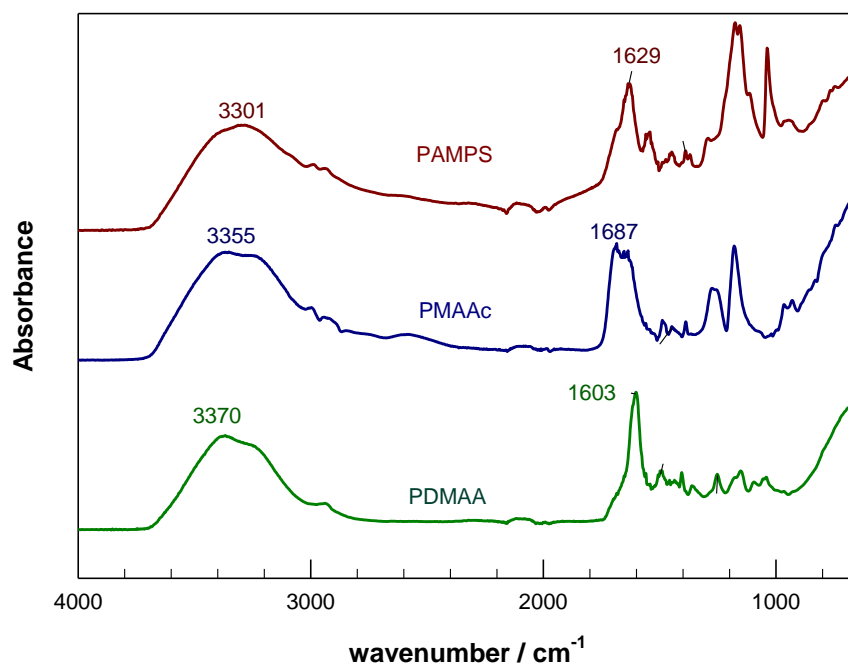


Figure S2. FTIR spectra of PAMPS, PMAAc, and PDMAA physical hydrogels formed at $w = 50$ wt % under identical conditions as described in the text.

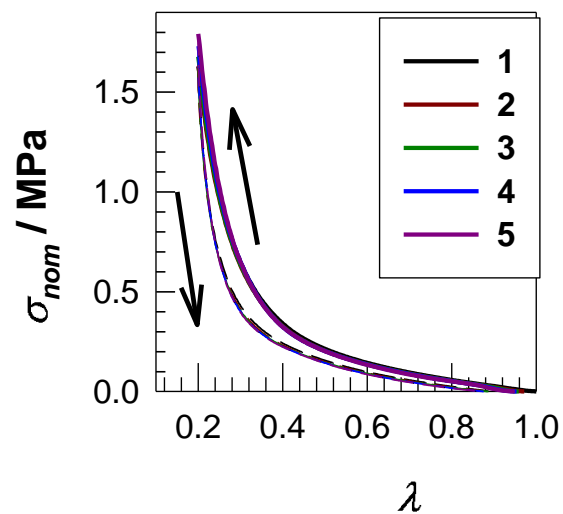


Figure S3. Five successive compressive cycles with a waiting time of 1 min between cycles. The cycle numbers are indicated. $w = 50$ wt %.

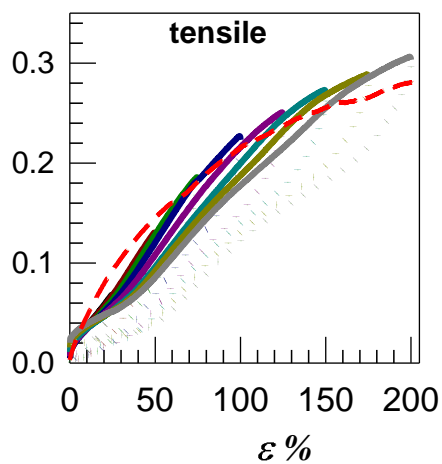


Figure S4. Eight successive tensile cycles for the hydrogels prepared at $w = 40$ wt %. ϵ_{\max} is increased from 25 to 200% with steps 25%. The dashed red curve represents the stress-strain curve of the virgin sample. $\dot{\epsilon} = 1 \text{ min}^{-1}$.

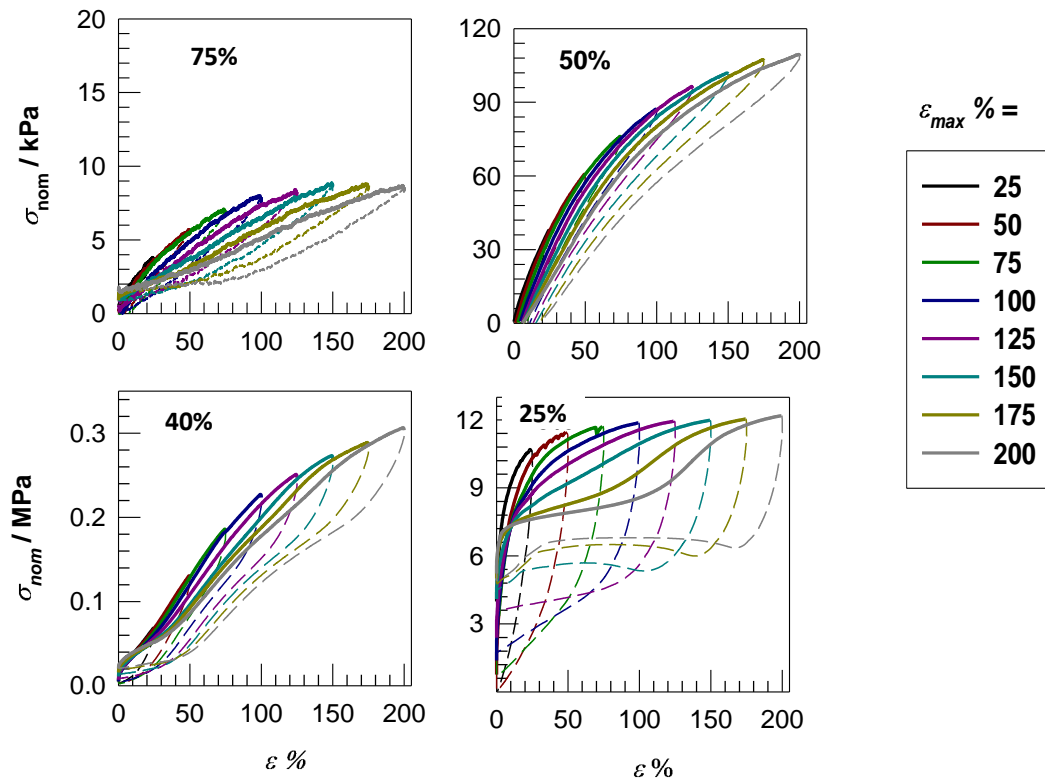


Figure S5. Eight successive tensile cycles for the hydrogels prepared at various w as indicated. ϵ_{max} is increased from 25 to 200% with steps 25%. $\dot{\epsilon} = 1 \text{ min}^{-1}$.